Tuning Riboflavin Derivatives For Photodynamic Inactivation of Pathogens

Ljiljana Fruk (lf389@cam.ac.uk)
University of Cambridge
Leander Crocker
University of Cambridge
Ju Hyun Lee
University of Cambridge
Suraj Mital
University of Cambridge
Gabrielle Mills
University of Cambridge
Sina Schack
University of Cambridge
Andrea Bistrovic-Popov
University of Cambridge
Christoph Franck
University of Cambridge
Ioanna Mela
University of Cambridge
Clemens Kaminski
University of Cambridge
Graham Christie
University of Cambridge

Article

Keywords: pathogen, Photodynamic, derivatives

Posted Date: November 29th, 2021

DOI: https://doi.org/10.21203/rs.3.rs-1111998/v1

Tuning Riboflavin Derivatives for Photodynamic Inactivation of Pathogens

Abstract

The development of effective pathogen reduction strategies is required due to the rise in antibiotic-resistant bacteria and zoonotic viral pandemics. Photodynamic inactivation (PDI) of bacteria and viruses is a potent reduction strategy that bypasses typical resistance mechanisms. Naturally occurring riboflavin has been widely used in PDI applications due to efficient light-induced reactive oxygen species (ROS) release. By rational design of its core structure to alter (photo)physical properties, we obtained derivatives capable of outperforming riboflavin's visible light-iinduced PDI against *E. coli* and a SARS-CoV-2 surrogate, revealing functional group dependency for each pathogen. Bacterial PDI was influenced mainly by guanidino substitution, whereas viral PDI increased through bromination of the flavin. These observations were related to enhanced uptake and ROS-specific nucleic acid cleavage mechanisms. Trends in the derivatives' toxicity towards human fibroblast cells were also investigated to assess viable therapeutic derivatives and help guide further design of PDI agents to combat pathogenic organisms.

Introduction

Riboflavin and its derivatives, flavin mononucleotide (FMN) and flavin adenine dinucleotide (FAD) are organic cofactors found within enzymes involved in numerous biochemical pathways.[1,2] Due to their rich redox chemistry and ability to mediate a wide range of both oxidative and reductive organic transformations, flavin-containing enzymes are prominently used as biocatalysts.[3,4] Flavins are also involved in the regulation of photochemical pathways due to strong blue light absorption, which results in the generation of highly oxidising excited states that can elicit biological signalling events or responses.[5–8] This photoexcitation process has been exploited in a number of photocatalytic applications, whereby modification of the flavin chromophore can enable the formation of high potential oxidative and reductive intermediates to afford useful synthetic methodology.[9–11]

Another application in which photoexcitation is utilised to generate reactive intermediates is within photodynamic inactivation (PDI) of pathogens. In this technique, a photosensitiser (PS) such as riboflavin, is employed to generate a burst of reactive oxygen species (ROS) in the vicinity of a particular pathogen in order to cause irreversible damage that leads to inactivation.[12,13] Due to the rapid onset and non-specificity of PS-induced ROS release, conventional mechanisms of pathogen resistance through specific efflux pumps or detoxification pathways can be avoided.[14] Therefore, PDI of pathogens is a versatile and effective strategy that has the potential to help combat increasing antibiotic-resistant bacteria strains,[14,15] and ongoing zoonotic viral pandemics.[16]

Mechanistically, PDI of a pathogen is initiated by excitation of a PS with a suitable wavelength of light (hv_{ex}) which generates an excited singlet state (S_1). This excited state can either fluoresce (hv_{em}) back to its ground state (S_0) or undergo intersystem crossing (ISC) to an excited triplet state (T_1), typically characterised by a longer lifetime (**Figure 1**). This excited triplet state PS can interact with substrate such as an amino acid residue or nucleobase to form an oxidised substrate and reduced PS that subsequently reduces oxygen to superoxide ($O_2^{\bullet-}$) (Type I reaction, **Figure 1**).[17] Superoxide is produced under oxidative stress naturally and is an important factor of cell signalling pathways.[18] Both prokaryotic and eukaryotic cells contain superoxide dismutase (SOD) enzymes in order to mitigate superoxide's cytotoxic effects.[17,18] Other types of ROS can be formed in Type I reactions such as H_2O_2 and hydroxyl radicals ($^{\bullet}OH$), however catalase and glutathione can neutralise these species respectively.[18]

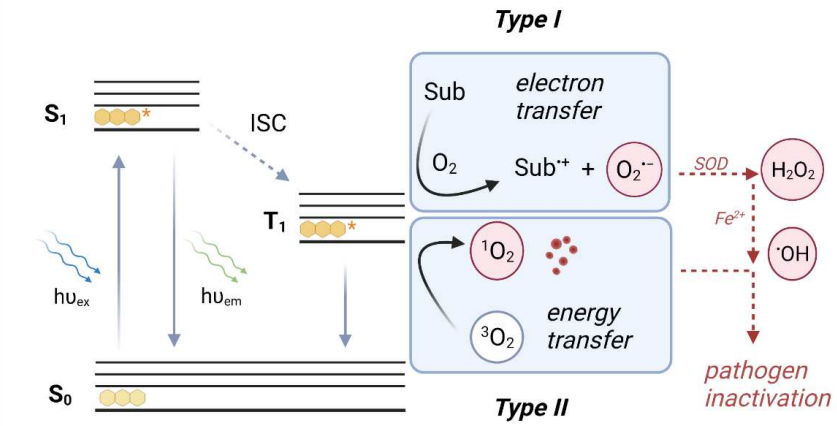

Figure 1. Mechanism of photosensitised reactive oxygen species (ROS) formation that enables inactivation of pathogens. ISC = intersystem crossing, Sub = substrate, SOD = superoxide dismutase.

Type II reactions lead to the formation of singlet oxygen ($^1O_2$), a highly cytotoxic ROS that non-selectively oxidises biomolecules such as nucleic acids, proteins and lipids in order to inactivate the pathogen.[17,18] Singlet oxygen formation occurs through the interaction of the excited triplet state PS with ground state triplet oxygen ($^3O_2$, **Figure 1**). The efficiency of the light absorption that leads to this event can be quantified through the measurement of the singlet oxygen quantum yield (Φ_Δ). Effective defence mechanisms against singlet oxygen have not evolved within non-photosynthetic microorganisms, hence it is considered key to PDI of bacterial and viral pathogens.[12,13,19]

Due to its excellent photosensitising properties, abundance and lack of toxicity, riboflavin has several applications within blood product sterilisation in combination with ultraviolet (UV) light for effective PDI of pathogens prior to transfusion.[20,21] More recently, it was shown to inactivate coronaviruses such as MERS and SARS-CoV-2.[22–24] Similarly, it has been reported that riboflavin and

FMN can inactivate bacteria,[25–27] cancer cells[28–30] and parasites[31] using either UV or blue (440-460 nm) light. Despite such promising studies, the design of flavin derivatives to understand structure-activity relationships towards PDI applications has not been explored, unlike prominent photosensitisers such as porphyrins,[32–34] phenothiaziniums,[35,36] and phenalen-1-ones.[37] Previously, it was shown that functionalisation of flavins with amino groups, which introduce positive charge, can enhance PDI against both Gram-negative and Gram-positive bacteria as well as endospores.[38–40] In general, cationic groups are known to improve the efficacy of PDI by coordination of the molecule to negatively charged phospholipid membranes. However, charge is not the only factor that contributes to the efficiency of PDI. For example, lipophilic flavin derivatives bearing multiple acetyl ester moieties have been shown to improve the efficacy against the *Leishmania major* parasite over analogous cationic ones, highlighting the importance of the cell membrane permeability.[31]

By considering the mechanism of PDI, as well as the biochemical structure of pathogens, we report the rational design of flavin derivatives (**F1-4**, **Figure 2a**) for pathogen inactivation. The prepared flavins demonstrate high efficacy and rapid inactivation of two model pathogens, a Gram-negative bacterium, *E. coli* BL21(DE3), and a SARS-CoV-2 surrogate, murine hepatitis virus A59 strain (MHV-A59)[41] under white light irradiation (400-700 nm). In addition, the toxicity of the derivatives towards human fibroblast cells (WI-38) is explored, revealing that clear structure-activity relationships can be observed relating to the functionality of derivatives.

Results and Discussion

Synthesis and characterisation of flavins

Flavins **F1-4** (**2A**) were prepared according to **Schemes S1** and **S2** (see **ESI**). Inspired by the classical amphiflavins developed by Trissel, Schmidt and Hemmerich,[42–46] we chose to include an alkyl chain (C_8) within the structure to improve phospholipid membrane incorporation. Additionally, the flavin chromophore itself was substituted with bromo groups in the case of **F3-4** in order to harness the heavy-atom effect that increases the rate of ISC from singlet to triplet excited states, thereby potentially enhancing photosensitised generation of singlet oxygen.[47] Heavy atom substitution has been shown to improve both the rate of ISC and the singlet oxygen quantum yield (Φ_Δ) in flavin derivatives used for synthetic photooxidation reactions.[48,49] Although the heavy-atom effect has been used to boost photodynamic efficacy for other PS dyes in PDI applications, it has not yet been explored for flavin derivatives.[50,51]

To afford both methylated (**F1-2**) and brominated derivatives (**F3-4**), a Boc-protected ethylene amino component was first installed to the methylated or brominated arene core prior to cyclisation

of the isoalloxazine ring system. Following N^3-alkylation with an octyl chain on the isoalloxazine, N-Boc protecting groups were removed to yield the amino-functionalised **F1** or **F3** that were subsequently converted to guanidino moieties to achieve **F2** or **F4** respectively (**Figure 2a**). Guanidino groups were chosen as they are known to increase membrane coordination and penetration through strong guanidinium-phosphate H-bonding. This interaction has been demonstrated to be key to the activity of arginine rich antimicrobial peptides[52] and cell penetrating peptides,[53–57] which we hypothesised would enhance PDI efficacy.

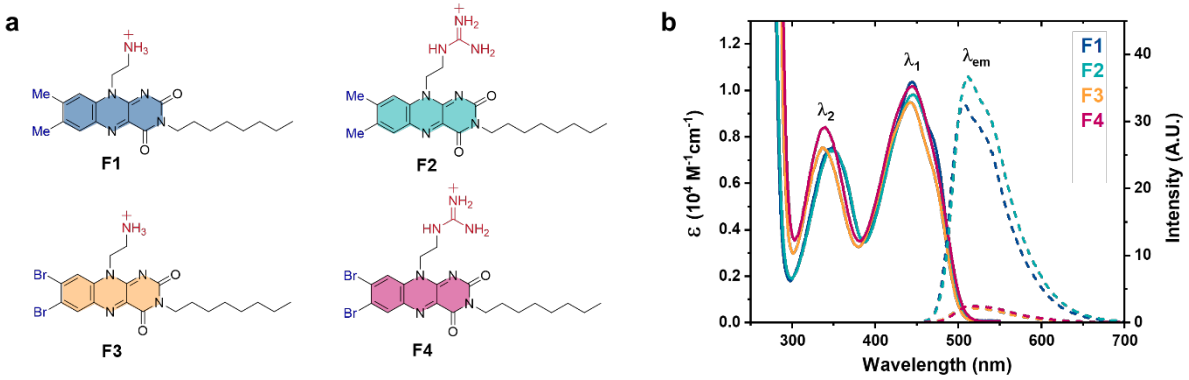

Figure 2. The structures and photophysical spectra of F1-4. a) Structures of flavins **F1-4** (counteranions = TFA^-), b) UV-Vis absorption (bold) and emission (dashed) spectra of **F1-4** in DMSO.

The UV-Vis absorption spectra of the flavins in DMSO revealed very similar absorption properties at the λ_1 ($S_0 \rightarrow S_1$) band but a blue shift of 10-13 nm for the higher energy λ_2 ($S_0 \rightarrow S_2$) bands of the brominated compounds (**F3** and **F4**) presumably due to the electron withdrawing effect of Br atoms (**Figure 2b**, **Table 1**). In terms of emission properties, the heavy-atom effect of bromination can be clearly observed with **F3** and **F4** exhibiting severely reduced emission intensity (Φ_F <2% in DMSO, **Table 1**) when compared to the methylated **F1** and **F2** (Φ_F = 13% and 14% respectively in DMSO, **Table 1**). This effect can also be observed when comparing the efficiency of $^1O_2$ production upon excitation, where brominated **F3** and **F4** demonstrate up to a 30% increase in activity over the methylated **F1** and **F2** in MeCN (**Table 1**), indicating their potential to be potent photodynamic agents. Despite this, **F1** and **F2** are still efficient $^1O_2$ photosensitisers comparable with riboflavin (Φ_Δ = 0.54 ± 0.07).[58] However, a smaller Φ_Δ value for guanidinylated **F4** (62%) is observed compared to aminated **F3** (85%) which could be explained by fast reverse ISC and/or solvent-dependent aggregation.

Table 1. Photophysical properties of flavins F1-4. λ_n = $S_0 \rightarrow S_n$ absorption band, λ_{em} = emission wavelength, ϕ_F = fluorescence quantum yield, ϕ_Δ = singlet oxygen quantum yield.

Flavin	λ_1 (nm)[a]	λ_2 (nm)[a]	λ_{em} (nm)[a]	ϕ_F[b]	ϕ_Δ[c]

F1	444	349	507	0.129 ± 0.012	0.49 ± 0.12
F2	446	350	512	0.141 ± 0.010	0.55 ± 0.10
F3	443	336	508	0.009 ± 0.013	0.85 ± 0.09
F4	444	340	513	0.011 ± 0.010	0.62 ± 0.10

[a] measured in DMSO

[b] calculated using riboflavin as the reference (φ_F = 0.226 ± 0.001 in DMSO)

[c] caluclated using $Ru(bpy)_3^{2+}$ as the reference (φ_Δ= 0.57 ± 0.06 in MeCN)

After successful synthesis and initial characterisation, we monitored the photostability of the compounds in PBS (1x, pH 7.4) which was used for PDI assays as distilled or ultrapure water destabilises bacterial cells[59] and coronaviruses through osmotic pressures,[60,61] thereby augmenting inactivation results. Flavins **F1-4** and riboflavin (100 µM in PBS) were therefore irradiated with a 6200K white LED light source (18W, 400-700 nm, see **ESI Figure S1** for emission spectrum) at an illuminance of $1x10^5$ lx (35 mW/cm^2 irradiance) to resemble typical daylight,[62] and the changes in their UV-Vis absorption were monitored over time (see **ESI**, **Figure S4**). For riboflavin, rapid photodecomposition (80%) was observed over 30 min irradiation which is known to be due to intramolecular dealkylation of the ribityl chain (**Figure S4a**, **S4b**).[63] This yields lumichrome as the major degradation product which can only act as a PS under UV-irradiation.[64] Amino-containing **F1** and **F3** exhibited around 40% and 60% degradation respectively after the same irradiation time (**Figure S4a**, **S4c** and **S4e**), whereas **F2** and **F4** degraded by approximately 10% and 30% respectively (**Figure S4a**, **S4d** and **S4f**). These findings corroborate previous work showing amino-containing flavins photodegradation in the presence of phosphate ions which resulted in diminished bacterial PDI efficiency,[40] however it appears that guanidino substitution improves photostability in this case. Interestingly, bromo-subtituted flavins show higher rates of photodegradation which could be explained by their higher Φ_Δ values resulting in greater $^1O_2$-induced degradation.[65]

Photodynamic inactivation of *E. coli*

Having observed clear trends in the photophysical properties of methylated and brominated derivatives, we were interested to see how this would affect the PDI efficacy of **F1-4** against pathogens. First, we investigated the inactivation of the Gram-negative bacterium, *E. coli* BL21(DE3). The cell envelope of Gram-negative bacteria presents a formidable barrier to antimicrobial compounds that consequently inhibits PDI efficacy compared to the analogous structure in Gram-positive bacteria.[66,67] Following an initial 20 min incubation of the flavin compounds with *E. coli* in PBS at various concentrations in the dark, the mixture was irradiated ($1x10^5$ lx) and the number of surviving colony forming units (CFUs) were determined. After 15 min (31.5 J/cm^2 light dose) of irradiation, no

inactivation was observed at 1 µM for either riboflavin or **F1-4**. At 10 µM approximately 1 log_{10} reduction of *E. coli* CFUs was observed for **F2** and a 2.8 log_{10} reduction in the presence of **F4** (**Figure 3a, Table S1**). At higher concentrations, this effect was greatly enhanced with both **F2** and **F4** exhibiting >6.0 log_{10} reduction of CFU/mL at 100 µM. From these data, it can be derived that 11 µM of **F4** and 42 µM of **F2** can achieve >3 log reduction (>99.9%) of bacterial load which is considered a minimum level of decontamination according to EMA guidance, whereas >6 logs is the highest.[68]

Interestingly, riboflavin and **F1** demonstrated no activity at 100 µM, whereas **F3** exhibited a 1.8 log_{10} reduction in bacterial load. To ensure effective PDI was occurring, the flavin compounds were incubated in the dark under the same experimental irradiation conditions (100 µM, 15 min) to reveal no bacterial toxicity (see ESI, **Figure S5**). The rate of *E. coli* inactivation over time was then monitored at a 100 µM flavin concentration revealing an extremely rapid reduction of CFUs in the presence of **F4**, facilitating >6.0 log_{10} reduction after just 5 min of irradiation (10.5 J/cm^2 light dose). Similarly, **F2** shows effective bactericidal activity with a 3.4 log_{10} reduction (>99.9%) after 5 min irradiation. A closer investigation into the speed of **F4**'s activity at 100 µM showed that after only 1 min of irradiation (2.10 J/cm^2 light dose) a 4.1 log_{10} reduction (>99.99%) of bacteria was achieved (**Figure 3b**).

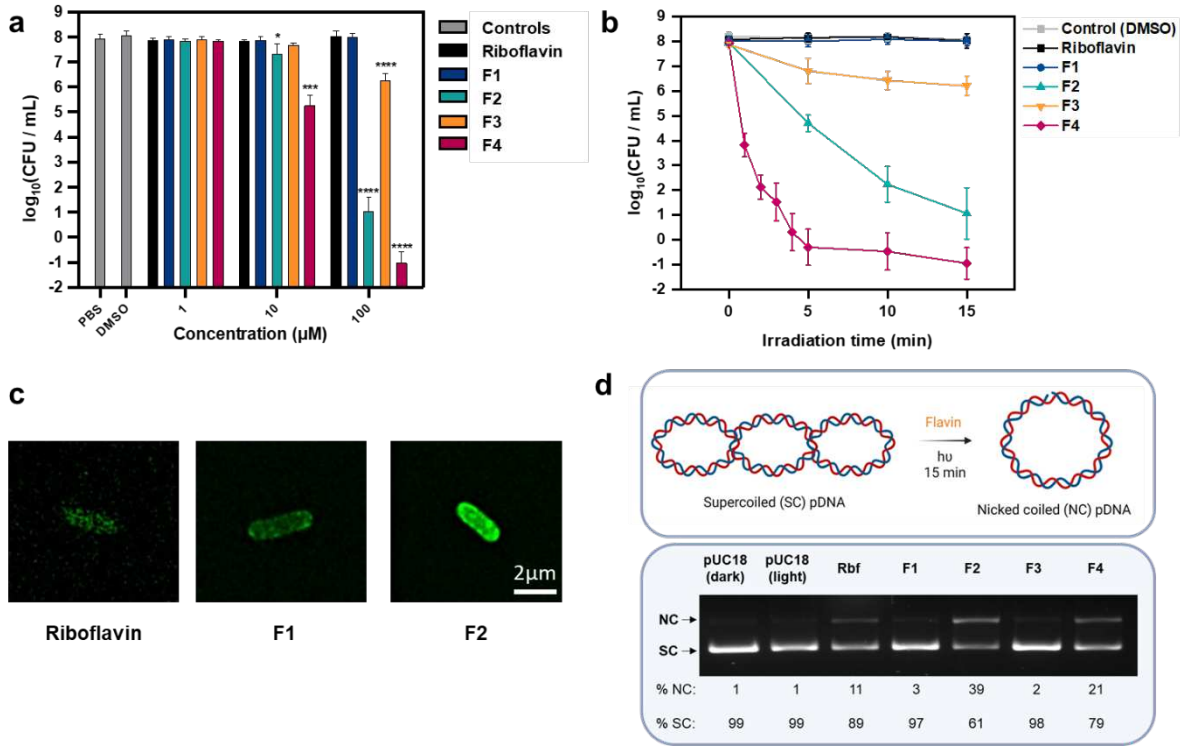

Figure 3. Photodynamic inactivation of *E. coli*. a) Photodynamic inactivation of *E. coli* BL21(DE3) incubated with various concentrations of flavins irradiated with white LED light (1x10^5 lx, 35 mW/cm^2)

for 15 min in PBS containing 0.5% DMSO. Data are expressed as the mean ± SD of three biological replicates. Significance levels are defined compared to PBS control as the following: * for p≤0.05, ** for p≤0.01, *** for p<0.001, and **** for p<0.0001. b) Time course of *E. coli* inactivation incubated with 100 µM of flavin irradiated with white LED light ($1x10^5$ lx, 35 mW/cm^2) for 15 min in PBS containing 0.5% DMSO. Data are expressed as the mean ± RE of three biological replicates. c) SIM images depicting the localisation of flavins in *E. coli* after incubation with 100 µM flavin. d) Agarose gel electrophoresis of pDNA (pUC18) following incubation with 10 µM flavin irradiated with white LED light ($1x10^5$ lx, 35 mW/cm^2) for 15 min in PBS containing 0.1% DMSO. Rbf = Riboflavin.

These data clearly show that the introduction of a guanidino moiety, as in the case of **F2** and **F4**, greatly increases the flavin's PDI efficacy against the bacterium when compared to amino-containing **F1** and **F3**. This may be attributed to better photostability in PBS, as well as the guanidino group facilitating better coordination to the cytoplasmic phospholipid membrane resulting in improved permeability and lipid peroxidation under irradiation.[69] In addition, the replacement of methyl substituents with bromines improves efficacy when the same cationic group is compared. This can be explained by more efficient generation of singlet oxygen, as predicted by their Φ_Δ values shown in **Table 1**. As a result, greater lipid and biomolecule oxidation can be achieved to inactivate the pathogen. It should also be noted that the inclusion of bromine atoms increases the lipophilicity of the molecule which can further improve cell membrane permeability and incorporation.[69] However, despite having the highest predicted Φ_Δ value (85%), **F3** did not outperform **F2** (Φ_Δ= 55%) which demonstrates the overarching impact of guanidino substitution.

To gain initial mechanistic insight, we investigated the cellular localisation of fluorescent riboflavin, **F1** and **F2** by structured illumination microscopy (SIM) (**Figure 3c**, see **ESI Figures S6-8**). After incubation with the flavin compounds (100 µM), large field of view images revealed marked differences in the number and degree of fluorescent bacterial populations (see **ESI Figures S6-8**). Although the exact quantification of flavin uptake was not possible due to uncharacterised optical properties in a complex biological environment, the qualitative comparison of **F2** and **F1** (which have similar Φ_F in DMSO), revealed a higher number of fluorescent bacteria with bright fluorescent intensity after incubation with **F2**, especially within membranes (**Figure 3c**, **Figure S6** and **S7**). This indicates that guanidino substitution does improve uptake, however the distribution of fluorescent intensity was not homogeneous across different bacterial cells which could be related to the amphiphilicity of **F2**, resulting in variable uptake due to aggregation (**Figure S6**). For hydrophilic riboflavin, very weak fluorescent populations were observed, most likely explained by the controlled transport of the compound through outer membrane porins of the bacterium and therefore unable to bind effectively

to the outer or cytoplasmic membranes (**Figure 3c, Figure S8**).[66] This therefore helps to explain the lack of PDI efficacy observed when using riboflavin.

Furthermore, we monitored the pDNA (pUC18) cleavage in the presence of the flavins (10 μM) under irradiation which indicated guanidino derivatives possess superior photocleavage ability (**Figure 3d**).[70] The photocleavage of supercoiled (SC) to nicked coiled (NC) pDNA structures was far enhanced for **F2** and **F4** (39% and 21% respectively) when compared to **F1** and **F3** (≤3%) after irradiation for 15 min (**Figure 3d**). This difference in activity could be explained by favourable guanidinium-phosphate interactions that increase the likelihood of electron transfer events between flavin and guanosine which are known to primarily contribute to DNA cleavage alongside $^1O_2$-mediated oxidation.[71,72] Therefore, even if the amino-flavin compounds diffuse into the cytoplasm, it is unlikely that damage to constituent nucleic acids would contribute to PDI of the pathogen.[73] Our control compound, riboflavin (**Rbf**) also exhibits photocleavage of the plasmid (11%) which has been reported previously,[71,72,74–76] however it is clear from the SIM data that, due to its hydrophilic nature and lack of cationic substituent, little cell uptake of the compound is achieved for this to contribute to PDI.

Collectively, this initial mechanistic study demonstrates that even in the case of increased singlet oxygen production, the key component to achieve effective Gram-negative bactericidal activity under irradiation is the presence of the guanidino group, which facilitates enhanced cell uptake and nucleic acid degradation.

Photodynamic inactivation of murine hepatitis virus (MHV-A59)

Encouraged by the identification of such highly effective guanidino-flavins for bacterial inactivation, we were interested to see if the trend would be similar for coronaviruses, specifically, the SARS-CoV-2 surrogate, murine hepatitis virus A59 strain (MHV-A59).[4]> It has already been demonstrated that riboflavin can effectively inactivate both enveloped and non-enveloped viruses in blood products using UV light,[20–24] but much lower efficacy was observed using visible light ($0.4x10^5$ lx, 0.5-2 h) against hepatitis B virus (HBV).[77,78] In order to evaluate possible applicability towards topical infection treatment and pathogen-inactivating surface coatings or textiles,[79–82] we used an *in vitro* $TCID_{50}$ assay to evaluate the viral titre of MHV-A59 through inoculation into murine fibroblast 17Cl-1 cells after irradiation at varying concentrations of flavin in PBS. The cytotoxicity of the flavins towards this cell line was first investigated by 24 h incubation MTS assay allowing us to obtain a working concentration range of ≤10 μM for the *in vitro* $TCID_{50}$ assay to evaluate viral PDI efficacy (see **ESI Figures S9** and **Table S3** for 17Cl-1 cytotoxicity data).

We started our investigation by varying the concentration of flavin (1-10 µM in PBS) with 10 min of white LED exposure (21.0 J/cm^2 light dose, **Figure 4a**). Even at 1 µM, the brominated guanidino flavin **F4** demonstrated a 3.8 $\log_{10}$ reduction in viral titre, while **F2** and **F3** showed 2.1 $\log_{10}$ reduction (**Figure 4a**, **Table S3**). It should be noted that reductions of the order of 4 logs or more (>99.99%) are considered highly effective by EMA guidance and that a >1 $\log_{10}$ reduction in necessary to be considered reliable.[83] At the same concentration, riboflavin achieved a 1.2 $\log_{10}$ reduction in titre, however **F1** showed no effect under these conditions. Nevertheless, the activity of all flavins improved by the increase of their concentrations resulting in viral load reductions of >99.9% in the presence of riboflavin or **F2**, and >99.99% with **F3** or **F4** at 5 µM. Further increase in concentration (to 10 µM) only substantially improved virucidal activity for **F4** (>5 $\log_{10}$). The irradiation time was then explored for 10 µM flavin to reveal high degrees of inactivation (≥5 $\log_{10}$) for **F2**, **F3** and **F4** when irradiated for 15 min (31.5 J/cm^2 light dose) whereas shorter irradiation times (5 min, 10.5 J/cm^2 light dose) still provided efficient inactivation of MHV-A59 ≥3 $\log_{10}$ steps using those same flavins (**Figure 4b**). It should be noted that variability within all experiments was noticeably high which is typical for $TCID_{50}$ assays.[84,85] However, no reliable log reduction of MHV-A59 was observed when irradiated without flavin in PBS containing 0.1% DMSO (**Figure 4b**). To confirm that the mechanism of viral inactivation by the flavins was dependent on light, dark control experiments (10 µM, 10 min incubation) resulted in no effective virucidal activity being observed (>1 $\log_{10}$ reduction, **Figure 4c**).[83]

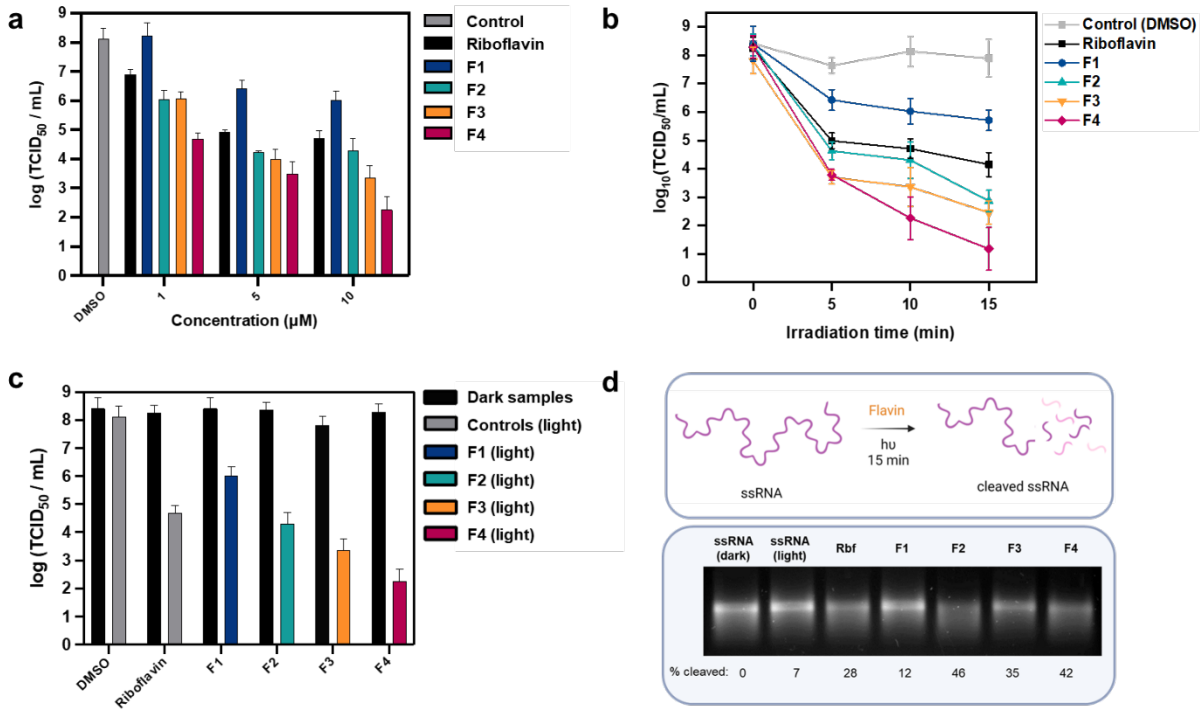

Figure 4. Photodynamic inactivation of murine hepatitis virus (MHV-A59). a) Photodynamic inactivation of murine hepatitis virus A59 strain (MHV-A59) incubated with various concentrations of

flavins irradiated with white LED light (1x10^5 lx, 35 mW/cm^2) for 10 min in PBS containing 0.1% DMSO. Data are expressed as the mean ± SD of three biological replicates. b) Time course of MHV-A59 inactivation incubated with 10 µM of flavin irradiated with white LED light (1x10^5 lx, 35 mW/cm^2) for 15 min in PBS containing 0.1% DMSO. Data are expressed as the mean ± RE of three biological replicates. c) Photodynamic inactivation of MHV-A59 incubated with 10 µM of flavin compound irradiated with white LED light (1x10^5 lx, 35 mW/cm^2) or incubated in the dark for 15 min in PBS containing 0.1% DMSO. Data are expressed as the mean ± SD of three biological replicates. d) Agarose gel electrophoresis of ssRNA following incubation with 10 µM flavin irradiated with white LED light (1x10^5 lx, 35 mW/cm^2) for 15 min in PBS containing 0.1% DMSO. Rbf = Riboflavin.

The activity of the flavin derivatives towards viral inactivation show a different trend than previously observed with our model bacterium. For example, in the presence of riboflavin under the same conditions, effective PDI of MHV-A59 was measured whereas there was no activity towards *E. coli*. Therefore, it can be assumed that the requirements for a PS to interact and/or diffuse through the coronavirus membrane are less dependent on lipophilicity or the presence of cationic charge. Despite this, our flavin derivatives again show that guanidino group incorporation improves antiviral PDI activity when compared to amino groups. However, bromination now seems to play a more important role in viral deactivation as brominated amino **F3** outperformed methylated guanidino **F2**.

To try and explain our findings, we investigated the interaction of the flavins with RNA to elucidate how its light-induced cleavage could lead to coronavirus inactivation.[8]> A model ssRNA (~1k nt) was irradiated (1x10^5 lx) in the presence of 10 µM flavin in PBS for 15 min and the extent of cleavage was observed *via* agarose gel electrophoresis (**Figure 4d**). It was observed that **F1** exhibits the least RNA photocleavage (12%) whereas riboflavin shows greater activity (28%) which corroborates the result of viral inactivation and confirms previous findings.[87–89] Similar to our results with pDNA, guanidino-containing **F2** and **F4** show the best photocleavage ability (46% and 42% respectively). Interestingly, **F3** also exhibits effective cleavage of RNA (35%) which was not observed in the case of pDNA (**Figure 3d**). This can be rationalised by the mechanism of flavin-mediated RNA photocleavage which has been previously shown to depend more upon $^1O_2$ oxidation than electron transfer events between flavin and nucleobase.[87–89] Taken together, it can be concluded that efficient $^1O_2$ production is key to viral PDI using flavin derivatives.

***In vitro* toxicity towards human cells**

Finally, before considering the applications of our flavin derivatives for PDI of topical pathogen infections, surface coatings or textiles, we investigated their impact on human cells. In general, an ideal photosensitiser for these applications should show no cytotoxic effects on human cells in the

dark and limited effects given the same irradiation conditions used for inactivation of the target pathogen, also referred to as a therapeutic window.[12] Accordingly, the inherent cytotoxicity of the flavins was evaluated through incubation with human lung fibroblast cells (WI-38). A 24 h MTS assay was used to calculate inhibitory concentration values (IC_{50}) of >100 µM for riboflavin and guanidino-functionalised **F2** and **F4** which can therefore be considered as non-toxic (**Figure 5a**, **Table S4**). On the other hand, amino-functionalised **F1** and **F3** had IC_{50} values of 96.1 µM and 30.9 µM respectively (**Table S4**). It has been shown previously that the cytotoxicity of amino-containing compounds may be derived from an increase in intracellular amine oxidase activity that induces excess oxidative stress leading to cell apoptosis.[90]

We then studied the light-induced toxicity of the flavins towards the WI-38 fibroblast cells by observing decreases in cell viability over irradiation time using an MTS assay (**Figure 5b**).[38] Interestingly, the cytotoxicity trends observed in the dark after 24h are reversed when exposed to light ($1x10^5$ lx) over shorter time periods. For example, after 15 min of irradiation, 10 µM of methylated guanidino **F2** induces ~75% reduction in cell viability. Under the same conditions, brominated guanidino **F4** exhibits less of an effect with ~20% reduction in cell viability. The degree of variability in these experiments could be attributed to the amphiphilic nature of the flavins leading to aggregation of the compounds in aqueous conditions. On the other hand, riboflavin, amino-functionalised **F1** and **F3** display no decrease in cell viability over 15 min irradiation, which supports previous findings.[38,39] These data show that despite being non-toxic to the cells in the dark, the guanidino-functionalised flavins can induce cytotoxicity upon irradiation most likely through similar mechanisms discussed for pathogens. It is our ongoing work to understand the differences in light induced cytotoxicity that were observed between methylated and brominated guanidino flavin derivatives. Nevertheless, **F4** could be suitable for further PDI applications thanks to effective bacterial and viral inactivation (>3 log_{10} reduction after 15 min irradiation at 11 µM and 1 µM respectively) coupled with low toxicity to human fibroblast cells under the same conditions or in the dark.

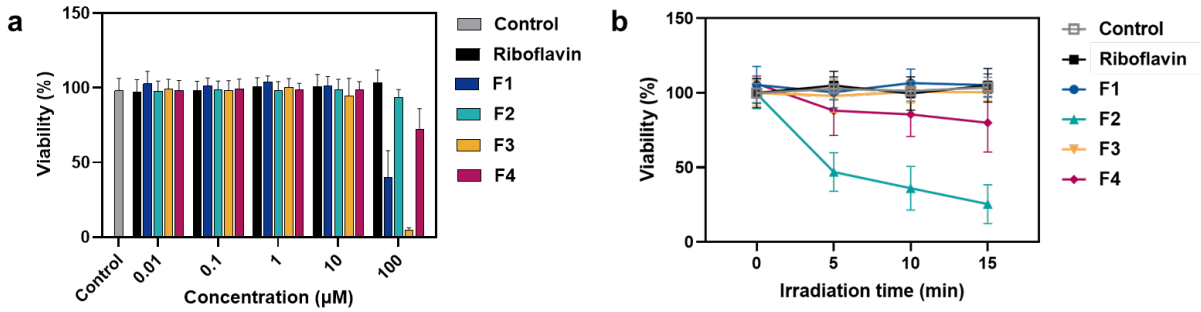

Figure 5. *In vitro* toxicity of F1-4 towards human cells. a) In vitro cytotoxicity effect of **F1–4** and riboflavin on WI-38 cells after 24 h incubation determined by MTS assay. Data are expressed as the

mean ± SD of three biological replicates. b) Light-induced toxicity of WI-38 cells treated with **F1**–**F4** and riboflavin (10 μM) irradiated for 0-15 min with 1x10^5 lx white LED light. Data are expressed as the mean ± SD of three biological replicates. Control = 0.1% DMSO in PBS.

Conclusion

In summary, we have rationally designed a set of flavin derivatives containing functional groups that significantly improve visible light photodynamic inactivation of pathogens. By incorporating a guanidino moiety into the flavin structure (**F2** and **F4**), the inactivation efficacy against Gram-negative bacteria, *E. coli* BL21(DE3) in PBS, was remarkably enhanced compared to natural riboflavin and amino variants (**F1** and **F3**). This was justified by enhanced cell uptake and pDNA cleavage facilitated by this group. Bromination of the structure (**F3** and **F4**) improved singlet oxygen production *via* the heavy-atom effect which generally led to improved PDI of *E. coli*, however the incorporation of a guanidino substituent dominated the outcome. Very effective inactivation was achieved with **F4**, whereby 1 min of visible irradiation (2.10 J/cm^2 light dose) reduced the bacterial load by >4 log_{10} steps.

It was found that less selectivity was placed upon the presence of a guanidino moiety when evaluating the PDI against the SARS-CoV-2 surrogate, MHV-A59 in PBS. This was evidenced by brominated amino **F3** having a higher efficacy compared to methylated guanidino **F2** which was attributed to greater RNA cleavage *via* $^1O_2$ oxidation. The highest viral PDI was achieved by **F4** where >4 log_{10} reduction in titre was achieved after 10 min of visible irradiation (21.0 J/cm^2 light dose) in the presence of 5 μM compound. Toxicity studies using the novel flavins towards human fibroblast cells (WI-38) further confirmed that **F4** could be a suitable candidate for PDI applications against both bacteria and viruses.

Overall, we hope this study inspires further exploration of riboflavin's structure to design new generations of photosensitiser compounds to treat topical bacterial or viral infections, enabling the design of antipathogenic surface coatings, as well as fabrics capable of efficient visible light pathogen inactivation.[79–82]

Methods

All experimental methods including synthesis, characterisation and PDI assays can be found in the **Supplementary Information**.

Data availability

The data that support the findings of this study are available from the corresponding author upon reasonable request.

References

1. Walsh, C. Flavin Coenzymes: At the Crossroads of Biological Redox Chemistry. *Acc. Chem. Res.* **13**, 148–155 (1980).

2. Massey, V. The chemical and biological versatility of riboflavin. in *Biochemical Society Transactions* vol. 28 283–296 (2000).

3. Walsh, C. T. & Wencewicz, T. A. Flavoenzymes: Versatile catalysts in biosynthetic pathways. *Natural Product Reports* vol. 30 175–200 (2013).

4. Baker Dockrey, S. A. & Narayan, A. R. H. Flavin-dependent biocatalysts in synthesis. *Tetrahedron* **75**, 1115–1121 (2019).

5. Kennis, J. T. M. & Mathes, T. Molecular eyes: Proteins that transform light into biological information. *Interface Focus* vol. 3 (2013).

6. Cashmore, A. R. Cryptochromes: Enabling plants and animals to determine circadian time. *Cell* vol. 114 537–543 (2003).

7. Masuda, S. Light detection and signal transduction in the BLUF photoreceptors. *Plant and Cell Physiology* vol. 54 171–179 (2013).

8. Losi, A. & Gärtner, W. Solving Blue Light Riddles: New Lessons from Flavin-binding LOV Photoreceptors. *Photochemistry and Photobiology* vol. 93 141–158 (2017).

9. König, B., Kümmel, S., Svobodová, E. & Cibulka, R. Flavin photocatalysis. *Phys. Sci. Rev.* **3**, (2019).

10. Graml, A., Neveselý, T., Jan Kutta, R., Cibulka, R. & König, B. Deazaflavin reductive photocatalysis involves excited semiquinone radicals. *Nat. Commun.* **11**, 1–11 (2020).

11. Pokluda, A. *et al.* Robust Photocatalytic Method Using Ethylene-Bridged Flavinium Salts for the Aerobic Oxidation of Unactivated Benzylic Substrates. *Adv. Synth. Catal.* **363**, 4371–4379 (2021).

12. Cieplik, F. *et al.* Antimicrobial photodynamic therapy–what we know and what we don't. *Critical Reviews in Microbiology* vol. 44 571–589 (2018).

13. Wiehe, A., O'brien, J. M. & Senge, M. O. Trends and targets in antiviral phototherapy. *Photochem. Photobiol. Sci.* **18**, 2565–2612 (2019).

14. Maisch, T. Resistance in antimicrobial photodynamic inactivation of bacteria. *Photochem.*

Photobiol. Sci. **14**, 1518–1526 (2015).

15. Wainwright, M. *et al.* Photoantimicrobials—are we afraid of the light? *The Lancet Infectious Diseases* vol. 17 e49–e55 (2017).

16. Sabino, C. P. *et al.* Light-based technologies for management of COVID-19 pandemic crisis. *Journal of Photochemistry and Photobiology B: Biology* vol. 212 111999 (2020).

17. Baptista, M. S. *et al.* Type I and Type II Photosensitized Oxidation Reactions: Guidelines and Mechanistic Pathways. *Photochemistry and Photobiology* vol. 93 912–919 (2017).

18. Schieber, M. & Chandel, N. S. ROS function in redox signaling and oxidative stress. *Curr. Biol.* **24**, R453–R462 (2014).

19. Glaeser, J., Nuss, A. M., Berghoff, B. A. & Klug, G. Singlet Oxygen Stress in Microorganisms. *Adv. Microb. Physiol.* **58**, 141–173 (2011).

20. Goodrich, R. P., Edrich, R. A., Li, J. & Seghatchian, J. The Mirasol^{TM} PRT system for pathogen reduction of platelets and plasma: An overview of current status and future trends. *Transfus. Apher. Sci.* **35**, 5–17 (2006).

21. Marschner, S. & Goodrich, R. Pathogen reduction technology treatment of platelets, plasma and whole blood using riboflavin and UV light. *Transfus. Med. Hemotherapy* **38**, 8–18 (2011).

22. Keil, S. D., Bowen, R. & Marschner, S. Inactivation of Middle East respiratory syndrome coronavirus (MERS-CoV) in plasma products using a riboflavin-based and ultraviolet light-based photochemical treatment. *Transfusion* **56**, 2948–2952 (2016).

23. Ragan, I., Hartson, L., Pidcoke, H., Bowen, R. & Goodrich, R. Pathogen reduction of SARS-CoV-2 virus in plasma and whole blood using riboflavin and UV light. *PLoS One* **15**, e0233947 (2020).

24. Keil, S. D. *et al.* Inactivation of severe acute respiratory syndrome coronavirus 2 in plasma and platelet products using a riboflavin and ultraviolet light-based photochemical treatment. *Vox Sang.* **115**, 495–501 (2020).

25. Liang, J. Y., Cheng, C. W., Yu, C. H. & Chen, L. Y. Investigations of blue light-induced reactive oxygen species from flavin mononucleotide on inactivation of E. coli. *J. Photochem. Photobiol. B Biol.* **143**, 82–88 (2015).

26. Wong, T. W., Cheng, C. W., Hsieh, Z. J. & Liang, J. Y. Effects of blue or violet light on the inactivation of Staphylococcus aureus by riboflavin-5'-phosphate photolysis. *J. Photochem.*

Photobiol. B Biol. **173**, 672–680 (2017).

27. Khan, S. *et al.* ROS mediated antibacterial activity of photoilluminated riboflavin: A photodynamic mechanism against nosocomial infections. *Toxicol. Reports* **6**, 136–142 (2019).

28. Edwards, A. M., Barredo, F., Silva, E., De Ioannes, A. E. & Becker, M. I. Apoptosis induction in nonirradiated human HL-60 and murine NSO/2 tumor cells by photoproducts of indole-3-acetic acid and riboflavin. *Photochem. Photobiol.* **70**, 645–649 (1999).

29. De Souza, A. C. S. *et al.* A promising action of riboflavin as a mediator of leukaemia cell death. *Apoptosis* **11**, 1761–1771 (2006).

30. Wolnicka-Glubisz, A., Pawlak, A., Insinska-Rak, M. & Zadlo, A. Analysis of photoreactivity and phototoxicity of riboflavin's analogue 3MeTARF. *J. Photochem. Photobiol. B Biol.* **205**, 111820 (2020).

31. Silva, A. V. *et al.* Riboflavin derivatives for enhanced photodynamic activity against Leishmania parasites. *Tetrahedron* **71**, 457–462 (2015).

32. Kou, J., Dou, D. & Yang, L. Porphyrin photosensitizers in photodynamic therapy and its applications. *Oncotarget* **8**, 81591–81603 (2017).

33. Wainwright, M. *Photosensitisers in biomedicine*. *Photosensitisers in Biomedicine* (Wiley Blackwell, 2009). doi:10.1002/9780470744956.

34. Tim, M. Strategies to optimize photosensitizers for photodynamic inactivation of bacteria. *J. Photochem. Photobiol. B Biol.* **150**, 2–10 (2015).

35. Wainwright, M. The development of phenothiazinium photosensitisers. *Photodiagnosis Photodyn. Ther.* **2**, 263–272 (2005).

36. Gollmer, A., Felgenträger, A., Bäumler, W., Maisch, T. & Späth, A. A novel set of symmetric methylene blue derivatives exhibits effective bacteria photokilling - A structure-response study. *Photochem. Photobiol. Sci.* **14**, 335–351 (2015).

37. Tabenski, I. *et al.* The impact of cationic substituents in phenalen-1-one photosensitizers on antimicrobial photodynamic efficacy. *Photochem. Photobiol. Sci.* **15**, 57–68 (2016).

38. Maisch, T. *et al.* Fast and effective photodynamic inactivation of multiresistant bacteria by cationic riboflavin derivatives. *PLoS One* **9**, (2014).

39. Eichner, A. *et al.* Fast and effective inactivation of Bacillus atrophaeus endospores using light-

activated derivatives of vitamin B2. *Photochem. Photobiol. Sci.* **14**, 387–396 (2015).

40. Eckl, D. B. *et al.* Interplay of phosphate and carbonate ions with flavin photosensitizers in photodynamic inactivation of bacteria. *PLoS One* **16**, e0253212 (2021).

41. Pendyala, B., Patras, A., Pokharel, B. & D'Souza, D. Genomic Modeling as an Approach to Identify Surrogates for Use in Experimental Validation of SARS-CoV-2 and HuNoV Inactivation by UV-C Treatment. *Front. Microbiol.* **11**, 2406 (2020).

42. Michel, H. & Hemmerich, P. Substitution of the flavin chromophore with lipophilic side chains: A novel membrane redox label. *J. Membr. Biol.* **60**, 143–153 (1981).

43. Schmidt, W. Fluorescence Properties of Isotropically and Anisotropically Embedded Flavins. *Photochem. Photobiol.* **34**, 7–16 (1981).

44. Michel, H., Schmidt, W. & Hemmerich, P. On the environment and the rotational motion of amphiphilic flavins in artificial membrane vesicles as studied by electron paramagnetic resonance spectroscopy. *Biophys. Chem.* **15**, 121–130 (1982).

45. Trissl, H. W. Studies on the incorporation of fluorescent pigments into bilayer membranes. *BBA - Biomembr.* **367**, 326–337 (1974).

46. Frehland, E. & Trissl, H. W. Fluorescence polarization in a planar array of pigment molecules: Theoretical treatment and application to flavins incorporated into artificial membranes. *J. Membr. Biol.* **21**, 147–173 (1975).

47. Koziar, J. C. & Cowan, D. O. Photochemical Heavy-Atom Effects. *Acc. Chem. Res.* **11**, 334–341 (1978).

48. Korvinson, K. A. *et al.* Improved Flavin-Based Catalytic Photooxidation of Alcohols through Intersystem Crossing Rate Enhancement. *J. Phys. Chem. A* **120**, 7294–7300 (2016).

49. Dang, C. *et al.* Flavin Dibromide as an Efficient Sensitizer for Photooxidation of Sulfides. *ACS Sustain. Chem. Eng.* **6**, 15254–15263 (2018).

50. Gorman, A. *et al.* In vitro demonstration of the heavy-atom effect for photodynamic therapy. *J. Am. Chem. Soc.* **126**, 10619–10631 (2004).

51. Zou, J. *et al.* BODIPY Derivatives for Photodynamic Therapy: Influence of Configuration versus Heavy Atom Effect. *ACS Appl. Mater. Interfaces* **9**, 32475–32481 (2017).

52. Zasloff, M. Antimicrobial peptides of multicellular organisms. *Nature* **415**, 389–395 (2002).

53. Tang, M., Waring, A. J., Lehrer, R. I. & Hong, M. Effects of guanidinium-phosphate hydrogen bonding on the membrane-bound structure and activity of an arginine-rich membrane peptide from solid-state NMR spectroscopy. *Angew. Chemie - Int. Ed.* **47**, 3202–3205 (2008).

54. Wang, F. *et al.* Recent progress of cell-penetrating peptides as new carriers for intracellular cargo delivery. *J. Control. Release* **174**, 126–136 (2014).

55. Sun, D., Forsman, J., Lund, M. & Woodward, C. E. Effect of arginine-rich cell penetrating peptides on membrane pore formation and life-times: A molecular simulation study. *Phys. Chem. Chem. Phys.* **16**, 20785–20795 (2014).

56. Wexselblatt, E., Esko, J. D. & Tor, Y. On guanidinium and cellular uptake. *J. Org. Chem.* **79**, 6766–6774 (2014).

57. Franck, C. O., Fanslau, L., Bistrovic Popov, A., Tyagi, P. & Fruk, L. Biopolymer-based Carriers for DNA Vaccine Design. *Angew. Chemie - Int. Ed.* **60**, 13225–13243 (2021).

58. Baier, J. *et al.* Singlet oxygen generation by UVA light exposure of endogenous photosensitizers. *Biophys. J.* **91**, 1452–1459 (2006).

59. Wood, J. M. Bacterial responses to osmotic challenges. *Journal of General Physiology* vol. 145 381–388 (2015).

60. Wang, X. W. *et al.* Study on the resistance of severe acute respiratory syndrome-associated coronavirus. *J. Virol. Methods* **126**, 171–177 (2005).

61. La Rosa, G., Bonadonna, L., Lucentini, L., Kenmoe, S. & Suffredini, E. Coronavirus in water environments: Occurrence, persistence and concentration methods - A scoping review. *Water Research* vol. 179 115899 (2020).

62. Michael, P. R., Johnston, D. E. & Moreno, W. A conversion guide: Solar irradiance and lux illuminance. *J. Meas. Eng.* **8**, 153–166 (2020).

63. Sheraz, M. A., Kazi, S. H., Ahmed, S., Anwar, Z. & Ahmad, I. Photo, thermal and chemical degradation of riboflavin. *Beilstein J. Org. Chem.* **10**, 1999–2012 (2014).

64. Tyagi, A. & Penzkofer, A. Absorption and emission spectroscopic characterization of lumichrome in aqueous solutions. *Photochem. Photobiol.* **87**, 524–533 (2011).

65. Huang, R., Choe, E. & Min, D. B. Kinetics for singlet oxygen formation by riboflavin photosensitization and the reaction between riboflavin and singlet oxygen. *J. Food Sci.* **69**, (2004).

66. Hancock, R. E. W. & Bell, A. Antibiotic uptake into gram-negative bacteria. *Curr. Top. Infect. Dis. Clin. Microbiol.* **2**, 21–28 (1989).

67. Malik, Z., Ladan, H. & Nitzan, Y. Photodynamic inactivation of Gram-negative bacteria: Problems and possible solutions. *J. Photochem. Photobiol. B Biol.* **14**, 262–266 (1992).

68. EMA. *Committee for Medicinal Products for Human use (CHMP) Committee for Medicinal Products for Veterinary use (CVMP) Guideline on the sterilisation of the medicinal product, active substance, excipient and primary container*. www.ema.europa.eu/contactTelephone+31 (2019).

69. Andreev, K. *et al.* Guanidino groups greatly enhance the action of antimicrobial peptidomimetics against bacterial cytoplasmic membranes. *Biochim. Biophys. Acta - Biomembr.* **1838**, 2492–2502 (2014).

70. Ohara, K. *et al.* Amine-guanidine switch: A promising approach to improve DNA binding and antiproliferative activities. *J. Med. Chem.* **50**, 6465–6475 (2007).

71. Kasai, H. & Yamaizumi, Z. Photosensitized Formation of 7,8-Dihydro-8-oxo-2′-deoxyguanosine (8-hydroxy-2′-deoxyguanosine) in DNA by Riboflavin: A Non Singlet Oxygen-Mediated Reaction. *Journal of the American Chemical Society* vol. 114 9692–9694 (1992).

72. Ito, K., Inoue, S., Yamamoto, K. & Kawanishi, S. 8-Hydroxydeoxyguanosine formation at the 5′ site of 5′-GG-3′ sequences in double-stranded DNA by UV radiation with riboflavin. *J. Biol. Chem.* **268**, 13221–13227 (1993).

73. Rapacka-Zdończyk, A. *et al.* Factors Determining the Susceptibility of Bacteria to Antibacterial Photodynamic Inactivation. *Front. Med.* **8**, 617 (2021).

74. Kino, K. & Saito, I. Product analysis of GG-specific photooxidation of DNA via electron transfer: 2-aminoimidazolone as a major guanine oxidation product [14]. *Journal of the American Chemical Society* vol. 120 7373–7374 (1998).

75. Frier, C., Mouscadet, J. F., Décout, J. L., Auclair, C. & Fontecave, M. Flavin-oligonucleotide conjugates: Sequence specific photocleavage of DNA. *Chem. Commun.* **5**, 2457–2458 (1998).

76. Yuan, Y. *et al.* Selective tumor cell death induced by irradiated riboflavin through recognizing DNA G-T mismatch. *Nucleic Acids Res.* **45**, 8676–8683 (2017).

77. Zhou, Z. Y. & Bi, X. X. Experimental studies on the inactivation of HBV in blood via riboflavin photochemical treatment. *Exp. Ther. Med.* **13**, 222–224 (2017).

78. Zhou, Z. Y. & Bi, X. X. Evaluation of the inactivation effect of riboflavin photochemical method on duck hepatitis B virus. *Exp. Ther. Med.* **15**, 751–754 (2018).

79. Hwang, G. B. *et al.* Photobactericidal activity activated by thiolated gold nanoclusters at low flux levels of white light. *Nat. Commun.* **11**, 1–10 (2020).

80. Eichner, A. *et al.* Novel photodynamic coating reduces the bioburden on near-patient surfaces thereby reducing the risk for onward pathogen transmission: a field study in two hospitals. *J. Hosp. Infect.* **104**, 85–91 (2020).

81. Tang, P. *et al.* Daylight-Induced Antibacterial and Antiviral Cotton Cloth for Offensive Personal Protection. *ACS Appl. Mater. Interfaces* **12**, 49442–49451 (2020).

82. Sun, G. *et al.* Daylight-induced antibacterial and antiviral nanofibrous membranes containing Vitamin K derivatives for personal protective equipment. *ACS Appl. Mater. Interfaces* **12**, 49430 (2020).

83. European Agency for the Evaluation of Medicinal Products. *Note for Guidance on Virus Validation Studies : the Design , Contribution and Interpretation of Studies Validating the Inactivation and Removal of Viruses Cpmp/Bwp/268/95*. *Committee for Proprietary Medicinal Products (CPMP)* vol. 0 http://www.ema.europa.eu/docs/en_GB/document_library/Scientific_guideline/2009/09/WC500003684.pdf (1996).

84. Malenovska, H. Virus quantitation by transmission electron microscopy, TCID50, and the role of timing virus harvesting: A case study of three animal viruses. *J. Virol. Methods* **191**, 136–140 (2013).

85. Smither, S. J. *et al.* Comparison of the plaque assay and 50% tissue culture infectious dose assay as methods for measuring filovirus infectivity. *J. Virol. Methods* **193**, 565–571 (2013).

86. Costa, L., Faustino, M. A. F., Neves, M. G. P. M. S., Cunha, Â. & Almeida, A. Photodynamic inactivation of mammalian viruses and bacteriophages. *Viruses* **4**, 1034–1074 (2012).

87. Burgstaller, P. & Famulok, M. Flavin-dependent photocleavage of RNA at G·U base pairs. *J. Am. Chem. Soc.* **119**, 1137–1138 (1997).

88. Liu, Y. *et al.* Photosensitized damage to telomere overhang and telomerase RNA by riboflavin. *Prog. Nat. Sci.* **18**, 401–404 (2008).

89. Zhao, Y. *et al.* Sequence-specific RNA photocleavage by single-stranded DNA in presence of

riboflavin. *Sci. Rep.* **5**, (2015).

90. Kappus, H. Oxidative stress in chemical toxicity. *Arch. Toxicol.* **60**, 144–149 (1987).

Conflicts of interest

The authors declare no competing interests.

Supplementary Files

This is a list of supplementary files associated with this preprint. Click to download.

- FLavinPDIESIDBRP.pdf